Bioelectromagnetics 41:136–147 (2020)

Phantom Model Testing of Active Implantable Cardiac Devices at 50/60 Hz Electric Field

Cihan Gerçek,[1,2] Djilali Kourtiche,[1]* Mustapha Nadi,[1] Isabelle Magne,[3] Pierre Schmitt,[1] Patrice Roth,[1] and Martine Souques[3]

[1]Institut Jean Lamour (UMR 7198), Universite de Lorraine-CNRS, Nancy, France
[2]Department of Design, Production and Management, University of Twente, Enschede, the Netherlands
[3]EDF SEM, Levallois-Perret, France

Exposure to external extremely low-frequency (ELF) electric and magnetic fields induces the development of electric fields inside the human body, with their nature depending on multiple factors including the human body characteristics and frequency, amplitude, and wave shape of the field. The objective of this study was to determine whether active implanted cardiac devices may be perturbed by a 50 or 60 Hz electric field and at which level. A numerical method was used to design the experimental setup. Several configurations including disadvantageous scenarios, 11 implantable cardioverter-defibrillators, and 43 cardiac pacemakers were tested in vitro by an experimental bench test up to 100 kV/m at 50 Hz and 83 kV/m at 60 Hz. No failure was observed for ICNIRP public exposure levels for most configurations (in more than 99% of the clinical cases), except for six pacemakers tested in unipolar mode with maximum sensitivity and atrial sensing. The implants configured with a nominal sensitivity in the bipolar mode were found to be resistant to electric fields exceeding the low action levels, even for the highest action levels, as defined by the Directive 2013/35/EU. Bioelectromagnetics. 2020;41:136–147. © 2020 Bioelectromagnetics Society

Keywords: **electric field; pacemaker; implantable cardiac defibrillator; extremely low frequency; active implantable medical device**

INTRODUCTION

The frequency of electrophysiological current in the human body ranges from direct current (DC) up to 200 Hz, which corresponds to the category of extremely low frequency (ELF) [Beebe, 1993]. At these frequencies, the electric and magnetic fields can be studied separately. When a human body is exposed to ELF electric fields, induced electric fields inside the body have the same frequency as the incident field and may induce a voltage on the same order of magnitude as biological signals. An electrocardiogram (ECG) has a frequency between 0.1 and 150 Hz [Webster and Clark, 2010], with a magnitude of 0.1–15 mV in a healthy adult [Jeremias and Brown, 2010]. The electromagnetic interference (EMI) is difficult to filter in the ELF frequency band for ECG devices [Schlimp et al., 2007] and active implantable cardiac devices (AICD) because of them being at the same frequency band as the biological signal.

There are different consequences of EMI, depending on the type of cardiac implant: pacemaker (PM) or implantable cardioverter-defibrillator (ICD). In addition to pacing, ICDs can deliver a high-voltage pulse, which might result in health risks in cases when EMI is detected as a pathological signal. Most device manufacturers guarantee the correct behavior of their AICDs up to 6 kV/m for 50 and 60 Hz electric fields.

Different guidelines have been established for the protection of humans exposed to electric fields from possible adverse health effects. For power line frequencies, the International Commission on Nonionizing Radiation Protection (ICNIRP) has set reference levels for public exposure at 5 kV/m for 50 Hz and 4.16 kV/m for 60 Hz [ICNIRP, 1998; ICNIRP, 2010]. The European Directive 2013/35/EU distinguishes occupational exposure into two action

Grant sponsor: Électricité de France (EDF) and Conseil Régional de Lorraine.

Conflicts of interest: None.

*Correspondence to: Djilali Kourtiche, Institut Jean Lamour, Université de Lorraine-CNRS-UMR 7198, 2 Allée André Guinier, BP 50840, 54011 Nancy Cedex, France. E-mail: djilali.kourtiche@univ-lorraine.fr

Received for review 27 November 2018; Accepted 18 December 2019

DOI:10.1002/bem.22245
Published online 5 January 2020 in Wiley Online Library (wileyonlinelibrary.com).

levels (ALs), as follows: low AL at 10 kV/m for 50 Hz and 8.33 kV/m for 60 Hz and high AL at 20 kV/m for 50 Hz and 16.66 kV/m for 60 Hz, respectively [Directive 2013/35/EU, 2013]. This directive defines workers bearing active medical implants as those who are at particular risk. The European standards from the EN 50527 series propose different methods to assess the risks [EN 50527-1, 2016; EN 50527-2-1, 2017; EN 50527-2-2, 2018]. These standards were established in the framework of the European Directive concerning workers with specific risks. Among the proposed methods of 50527-1, an in vitro study is a possible option. This type of provocative study is composed of two steps: (i) determination of the voltage on the AICD leads induced by the EMI, and (ii) reproduction of the EMI to test the AICD.

The induced electric field inside the human body cannot be measured accurately, and therefore the estimation of the induced voltage on the AICD leads is complex. For this reason, studies often make approximations on in vitro experiments or numerically investigate the amplitude of electric fields for each organ [Stuchly and Kavet, 2005; Napp et al., 2014]. In a previous paper, we described the in vitro approach applied to low-frequency magnetic fields [Katrib et al., 2013]. In vitro studies commonly use a rectangular phantom for magnetic field exposure. However, this rectangular shape cannot be used for electric field exposure in the present case due to the influence of the shape of the body on the induced electric field [International Electrotechnical Commission, 2007]. Exposure to a vertical electric field is the orientation setup that induces the maximum electric field inside the body; thus, this worst-case orientation is the only one considered in prior studies.

To experiment with the effects of electric field exposure, the phantom should be designed numerically, respecting the electric field induction or shaped like a real human body. Finnish research team worked with a male mannequin (1.93 m) filled with a solution (0.2 S/m) representing the mean value of conductivity and dielectric permittivity of the human tissue [Korpinen et al., 2012]. The phantom, containing a cardiac implant, was placed under high-voltage lines to analyze the in situ behavior of the AICD. Only 1 in 31 PMs showed a dysfunction at 7 kV/m in the unipolar sensing mode [Korpinen et al., 2012]. A similar test was repeated for 37 ICDs. Again, only one of them reacted improperly at 5.1 kV/m (bipolar mode) [Korpinen et al., 2014].

In collaboration with Hydro-Québec, the Montreal Heart Institute conducted in vitro tests in a high-voltage laboratory on 21 PMs and 19 ICDs [Dyrda et al., 2015]. Ultimately, the results indicated disruption of the AICDs at 1.5 kV/m in the worst-case configurations at 60 Hz. For a nominal configuration and bipolar mode, all PMs resisted to at least 8.6 kV/m, and all ICDs did the same to at least 2.9 kV/m [Dyrda et al., 2015]. These values were obtained from a grounded cylindrical human-size phantom exposed to an up-to-20 kV/m vertical electric field in a high-voltage hall.

The University of Aachen conducted in vivo studies by exposing patients implanted with Helmholtz coils to magnetic fields. Simultaneously, they injected a current defined by an empirical equation to simulate electric field exposure [Deno, 1977]. One-hundred and 10 patients with ICDs were exposed up to a 2.55-mT and 30-kV/m simulated electric field with electric current injections [Napp et al., 2014]. Results were that 39 ICDs configured to maximal sensitivity malfunctioned (one between 5 and 10 kV/m and 38 between 10 and 30 kV/m, respectively). The current injection method was validated by measuring induced voltage close to the heart in six volunteers and comparing the behavior of the implants in a laboratory exposure to a high-voltage electric field. The current injection method may underestimate the induced voltage by around 46% or more compared with the external electric field exposure method. The study injected 14 μA, regardless of the patient's height, for each kV/m, and their previous work in 2009 showed that the patient's radius influenced the induction [Joosten et al., 2009]. The authors concluded that public exposure levels do not disturb ICDs' functions. However, occupational environments may lead to false detection, especially since the atrial sensing mode is more susceptible [Napp et al., 2014].

Our in vitro study aims to operate as close as possible to an in vivo exploration. We employ computational methods to design a cost-effective test bench and phantom with the same induction as the heart area of a grounded, standing human [Gercek et al., 2017a]. In vitro tests will permit an increase in the field and elucidation of the exact value of the vertical electric field, causing the dysfunction. An in vitro study also permits exposure of AICDs to very high electric fields, which would be risky with patients in vivo.

MATERIALS AND METHODS

The design of the experimental bench and its phantom was created by numerical simulations to be able to get as close as possible to a real-world exposure scenario. We used Computer Simulation Technology (CST Studio Suite, Darmstadt, Germany) software, electromagnetism (EM), and low-frequency modules based on finite integration techniques [Weiland, 1977; Motrescu and van Rienen, 2005].

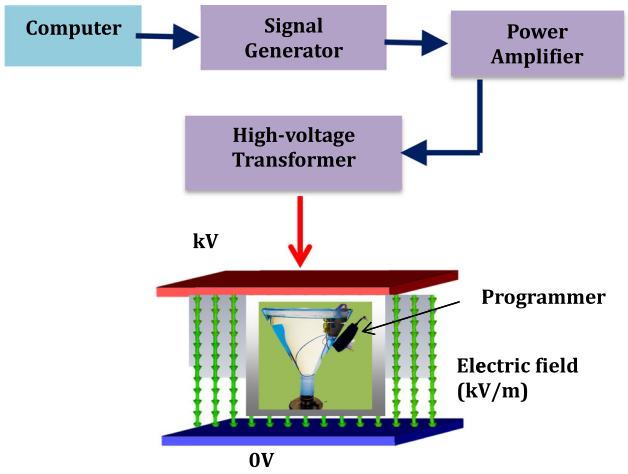

Fig. 1. Experimental setup: Composed of a voltage generator followed by a power amplifier and a high voltage transformer. The high voltage is applied to the exposure system.

EXPERIMENTAL BENCH

Figure 1 shows the experimental setup. The voltage of the upper plates was injected from a signal generator Agilent Keysight 33120A Programmable by Keysight VEE Pro (Keysight, Santa Rosa, CA), via a power amplifier (500 VA, 25 V, 40–400 kHz; KMP Electronics, Clamart, France), a transformer (24 V/220 V, 50–60 Hz), and a high-voltage transformer (209 V/60 kV, 20 mA, 50–60 Hz; Transfo Industrie, Gargenville, France). The other plate was grounded. The electric field was measured inside the plates using a field meter (ESM 100-FTT; Maschek, Bad Wörishofen, Germany) placed on an insulated tripod. The experimental chamber (where high voltages were put on the upper plate) was separated from the cockpit to prevent any risk to the operators and ensure the integrity of sensitive equipment. A safety system prevented anyone from entering the experimental chamber if the field was present and, conversely, the high voltage could not be applied if a person was present in the room. A screen connected to a camera (Panasonic WV-CP280/G CCTV, Osaka, Japan) showed the inside of the room as a double-check. The maximal levels of the electric field inside the test bench were 100 kV/m at 50 Hz and 83 kV/m at 60 Hz, respectively.

PHANTOM AND AICD

Results from an induced electric field in the heart using an anatomical human body model (with and without cardiac implant) were presented in the previous work (Fig. 2) [Gercek et al., 2017b]. The maximum induced field over the heart was calculated as 4 mV/m, and the mean induced electric field over the thorax was calculated as 0.8 mV/m (for an applied electric field of 1 kV/m). We intended to reproduce this induction for this study using a numerically designed phantom.

To design the experimental setup, we performed several numerical simulations with CST software (CST Studio Suite) on smaller-sized phantoms that could be placed between the plates (Fig. 2). The height of the phantom was 352 mm, which is equivalent to one-fifth of the human reference as defined by the International Commission on Radiological Protection in 2002 [Valentin, 2002]. The phantom was miniaturized to be able to position it between the test bench conductor planes. The top diameter of the glass funnel was chosen at a 300 mm radius to be similar to the human thorax circumference [IEC 62226-3-1, 2007]. For comparison, 8 out of 15 patients investigated in vivo, including the worst induction case, had a thorax circumference smaller than our phantom [Joosten et al., 2009]. By staying within the range of a human thorax circumference, the glass funnel could represent different cases of thorax circumference (by adjusting the fill level) and contain a properly positioned cardiac implant. The phantom reproduces an induced electric field of 0.8 mV/m in the mean value for the conic part, corresponding to a thorax induction of a human anatomical model [Gercek et al., 2017a,b]. For the cylindrical part, the phantom induces 4 mV/m, which gives a homogeneous distribution of the field suitable to position the implant probe. The latter represents the maximum induction of the anatomical human heart simulations [Gercek et al., 2017b]. Further detail and design methodology, technical details on the phantom, simulations of induction, and the positioning of the AICD box can be found in Gercek et al. [2017a].

As this phantom does not look like a human geometric phantom, the lead is meant to be positioned in a way that the field would be as homogeneous as possible so that a correlation could be drawn between anatomical induction and phantom induction [Gercek et al., 2017a]. Figure 2 shows the placement of the probe and the implant. The lead is attached not to modify the field but to have the same pattern for each experiment. We tested the same type of probe of different marks but did not find any significant difference; however, it was not possible to repeat all these tests over 54 AICD for 16 configurations and a significant number of different leads or trajectories of leads.

The induced voltages on AICDs obtained by the implanted whole-body simulation and implanted reduced phantom (one-fifth of the human body)

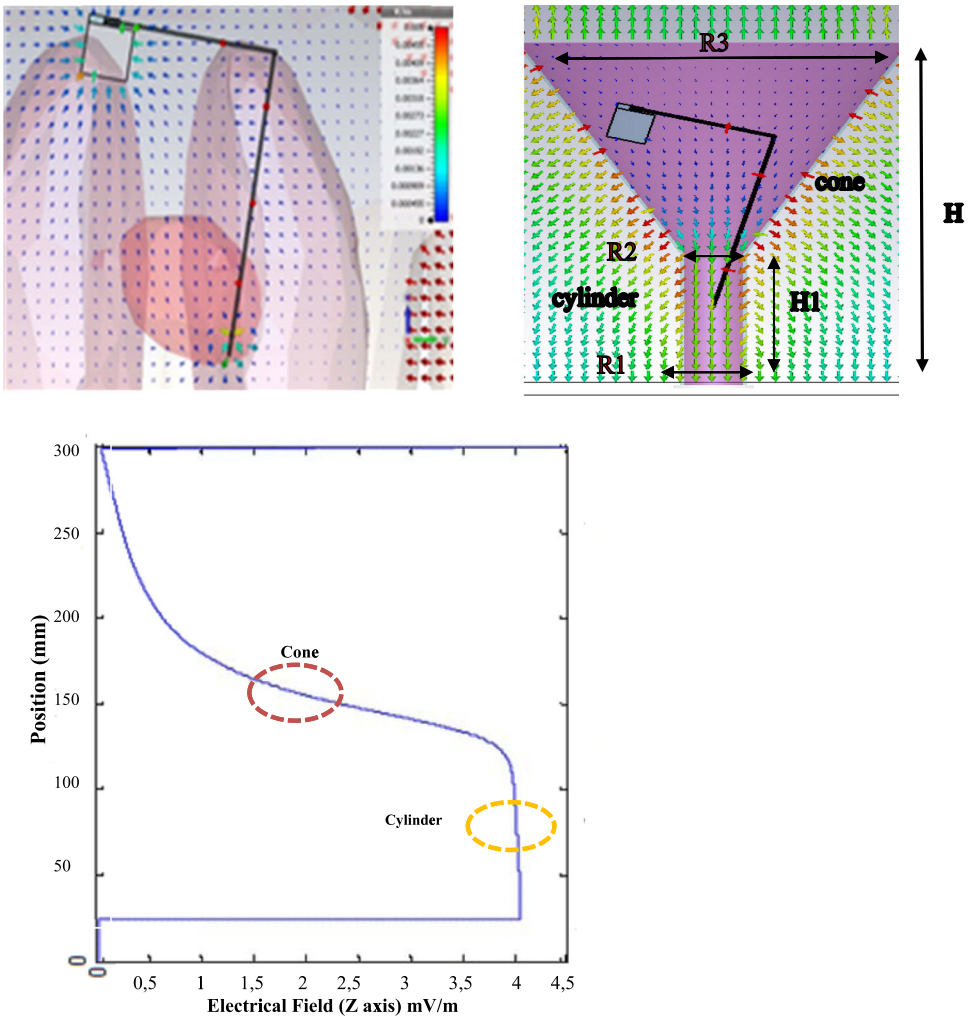

Fig. 2. This figure shows the simulation of the experimental phantom and the analogy with an implanted human torso. The cardiac implant is positioned in the cone area, and the cardiac probe (equipped with electrodes) is in the cylindrical portion where the electric field is constant. The dimensions of the phantom are H = 352 mm, H1 = 135 mm, R = 120 mm, R2 = 54 mm, and R3 = 300 mm.

allowed us to obtain a scaling factor of 2.45 in the case of unipolar detection and 2.48 for bipolar detection, respectively. The impact of 1 kV/m of phantom exposure from the implant would be equivalent to 2.45 kV/m of real exposure for a unipolar sensing mode and 2.48 kV/m for a bipolar sensing mode [Gercek et al., 2017a].

Figure 3 shows the exposure system and phantom used for the experimental part. The phantom was made of glass with a 3.3-mm thickness filled with 5 L of 0.2 S/m saline solution to reproduce the mean value of human tissues for 50 and 60 Hz, as mentioned by Gabriel et al. [2009].

The phantom is composed of a conical part and cylindrical part. To ensure proper grounding with the earth, a metallic sole was made of stainless steel to avoid any oxidation (saltwater). The sole was placed on the lower electrode, which previously had been polished. To ensure better contact, we added a braid of mass between the stopper and plate. The sole, connected to the ground, was then plugged into the cylindrical base. We selected a bottom large enough (R1 = 150 mm) to be able to maintain the phantom in a vertical position and connect it properly to the ground.

The dimensions of the phantom were height H = 352 mm, H1 = 135 mm, angle of the cone = 60°, R1 = 120 mm, R2 = 54 mm, and R3 = 300 mm, which points out the diameter of the solution and thorax circumference to be tested in our case. The cardiac implant was fixed on a Plexiglas support in the upper part of the cone. The electrodes were in the zone where the electric field was constant (Fig. 3).

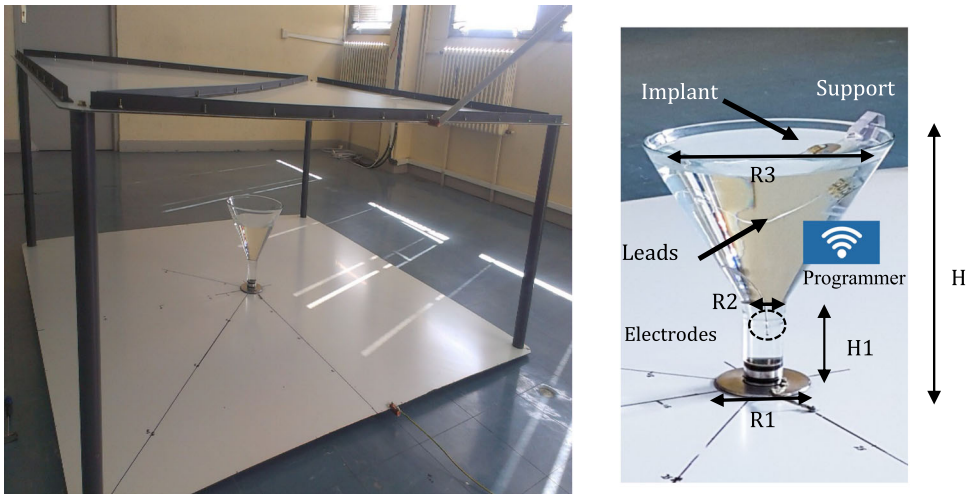

Fig. 3. This figure shows the exposure system and phantom used for the experimental part. The cardiac implant is fixed on a plexiglas support in the upper part of the cone. The electrodes are in the zone where the electric field is constant. Telemetry (programmer) was set to the communication position to interrogate the active implantable cardiac devices (AICD) inside the phantom. The phantom is composed of a conical part and a cylindrical part. The bottom of the cylindrical part in contact with the "ground" of the exposure system is closed by a metal plug of diameter R1. The dimensions of the phantom are: height is H = 352 mm, H1 = 135 mm, angle of the cone = 60°, R1 = 120 mm, R2 = 54 mm, and R3 = 300 mm, which points out the diameter of the solution and the thorax circumference to be tested in our case.

The responsiveness of explanted AICDs was checked by interrogating the state of the battery using telemetry. A passive-fixation lead was used for all ICDs, and an active fixation lead was used for all PMs. These leads were checked both by manual measurements and measurements done by the AICD once they were connected to the device.

The functionality of both the lead and implant were checked to determine whether they received the cardiac signal and if they could distinguish the pathological signals. All implants tested ($n = 54$) passed this review, including those with low battery power, as they proved good functioning. Telemetry messages, such as requesting a change of batteries, were ignored. The AICDs were still included in the test as the alert was only a warning about the need for changing out the AICD in the near future. The manufacturers assured that the AICDs were functioning well [CRDM Technical Services, 2014; Abbott, 2017]. The states of the AICDs are mentioned in Table 1.

Seventeen AICDs had almost run out of batteries at the time of the investigation. We noted that (contrary to the others) telemetry indicated some functions of these AICDs, which would not be effective with their remaining battery life. Therefore, we excluded 3 ICDs and 14 PMs, which are not mentioned further in this paper. For more information about the state of charge, one must refer to the guidance letters of relevant manufacturers [CRDM Technical Services, 2014; Abbott, 2017]. The list of AICDs tested is presented in Table 1.

Although 99% of PMs are generally used in bipolar mode, the unipolar mode also was tested. The maximum sensitivity and nominal sensitivity were set for unipolar and bipolar configurations, and the AICDs were exposed to 50 and 60 Hz separately. All the PMs were tested in ventricular-inhibited pacing mode (VVI) and atrial-inhibited pacing mode (AAI), which yielded 16 configuration cases for each implant. We applied the AAI mode of PMs so that some auricular tachycardia detection functions were activated. The AAI mode renders PMs more vulnerable, and therefore worst-case conditions can be fulfilled.

ICDs were tested at maximum sensitivity, with the worst configuration and nominal sensitivity at 50 and 60 Hz in bipolar mode only. All four cases were tested separately. We systematically tested VVI configuration for all ICDs, as they are the devices most commonly used for ventricular cases [Orgeron et al., 2017; Pavlicek et al., 2017; Tracy et al., 2013].

TEST PROCEDURE

AICDs were exposed to an electric field via the following five steps: (i) recording and checking the

TABLE 1. AICD Identification and Information

ID No.	Manufacturer	Model	Pacing mode	Detection rate (ppm)	Battery: V/V_{total}, State	Implantation date
ICD1	Medtronic	Concerto II CRT-D	VVI	200	2.94/2.63	29.07.2010
ICD2	Medtronic	Concerto II CRT-D	VVI	200	2.83/2.63	20.10.2010
ICD3	Medtronic	Concerto II CRT-D	VVI	200	2.73/2.63	26.10.2010
ICD4	Medtronic	Consulta CRT-D	VVI	200	2.61/2.63 EOS	11.05.2011
ICD5	Medtronic	Consulta CRT-D	VVI	200	2.69/2.63	16.03.2011
ICD6	Medtronic	Virtuoso II VR	VVI	200	2.98/2.63	3.06.2010
ICD7	Medtronic	Virtuoso II DR	VVI	200	2.62/2.63 RTT	16.02.2010
ICD8	Medtronic	Maximo VR	VVI	200	2.59/2.63 ERI	16.06.20XX
ICD9	Medtronic	Secura DR	VVI	200	Full	New
ICD10	St. Jude Medical	Atlas II VR	VVI	200	2.55	02.04.09
ICD11	St. Jude Medical	Atlas + HF	VVI	200	ERI	Demo
PM1	St. Jude Medical	Zephir XL DR 5826	AAI/VVI	180	2.78/2.45	27.03.09
PM2	St. Jude Medical	Zephir XL DR 5826	AAI/VVI	180	2,81	18.03.09
PM3	St. Jude Medical	Zephir XL DR 5826	AAI/VVI	180	2.78/2.45	20.04.08
PM4	St. Jude Medical	Identity ADx XL DR 5386	AAI/VVI	180	2.78/2.45	17.07.06
PM5	St. Jude Medical	Frontier II 5596	AAI/VVI	180	2.78/2.45	2.12.08
PM6	St. Jude Medical	Frontier II 5596	AAI/VVI	180	2.8/2.45	11.12.08
PM7	St. Jude Medical	Verity ADx XL SC 5056	AAI/VVI	180	2.78/2.45	06.07.06
PM8	St. Jude Medical	Integrity ADx XL DR 5366	AAI/VVI	180	2.72/2.45	–
PM9	St. Jude Medical	Identity ADx VDR 5480	AAI/VVI	180	2.72/2.45	15.05.07
PM10	St. Jude Medical	MicronyII SR +	AAI/VVI	180	2.78/2.45	–
PM11	Medtronic	Adapta L	AAI/VVI	180	2.68	26.01.07
PM12	Medtronic	Adapta L	AAI/VVI	180	2.76	29.08.11
PM13	Medtronic	Adapta L	AAI/VVI	180	2.75	31.03.08
PM14	Medtronic	Adapta L	AAI/VVI	180	2.72	27.01.12
PM15	Medtronic	Adapta L	AAI/VVI	180	2.77	26.08.09
PM16	Medtronic	Adapta L	AAI/VVI	180	2.74	04.06.12
PM17	Medtronic	Adapta L	AAI/VVI	180	2.65	02.03.07
PM18	Medtronic	Adapta L	AAI/VVI	180	2.74	07.09.10
PM19	Medtronic	Adapta (ADDR01)	AAI/VVI	180	2.75	04.01.12
PM20	Medtronic	Adapta (ADDR01)	AAI/VVI	180	2.75	08.12.10
PM21	Medtronic	Adapta (ADDR01)	AAI/VVI	180	2.74	28.10.09
PM22	Medtronic	Adapta (ADDR01)	AAI/VVI	180	2.76	09.02.10
PM23	Medtronic	Adapta (ADSR01)	AAI/VVI	180	2.71	16.08.10
PM24	Medtronic	Adapta (ADSR01)	AAI/VVI	180	2.68	03.05.10
PM25	Medtronic	Adapta (ADSR01)	AAI/VVI	180	2.68	18.11.10
PM25	Medtronic	Adapta (ADSR03)	AAI/VVI	180	2.73	11.12.12
PM26	Medtronic	Adapta (ADSR03)	AAI/VVI	180	2.71	19.10.10
PM27	Medtronic	Adapta S	AAI/VVI	180	2.61 ERI	31.08.10
PM28	Medtronic	EnPulse	AAI/VVI	180	2.67 ERI	30.05.05
PM29	Medtronic	EnPulse	AAI/VVI	180	2.66	12.10.05
PM30	Medtronic	EnPulse	AAI/VVI	180	2.66	22.03.07
PM31	Medtronic	INSYNC III model 8042	AAI/VVI	180	2.94	12.12.09
PM32	Medtronic	Adapta (ADDR03)	AAI/VVI	180	Full	New
PM33	Medtronic	Adapta (ADSR01)	AAI/VVI	180	Full	New
PM34	Vitatron (Medtronic)	T20SR model T20A1	AAI/VVI	180	2.75	18.06.07
PM35	Vitatron (Medtronic)	T20SR model T20A1	AAI/VVI	180	2.75	10.10.08
PM36	Vitatron (Medtronic)	T20SR model T20A2	AAI/VVI	180	2.75	20.06.10
PM37	Vitatron (Medtronic)	T20SR model T20A2	AAI/VVI	180	2.75	14.03.11
PM38	Vitatron (Medtronic)	G20SR model G20A1	AAI/VVI	180	2.74	10.07.12
PM39	Vitatron (Medtronic)	G20SR model G20A1	AAI/VVI	180	2.76	31.10.12
PM40	Vitatron (Medtronic)	C20SR model C20A3	AAI/VVI	180	2.75	29.11.05
PM41	Vitatron (Medtronic)	T70DR model T70A2	AAI/VVI	180	2.75	18.11.08
PM42	Vitatron (Medtronic)	G70DR model G70A1	AAI/VVI	180	2.76	11.07.12
PM43	Vitatron (Medtronic)	G70DR model G70A1	AAI/VVI	180	Full	New

AAI = atrial-inhibited pacing mode; VVI = ventricular-inhibited pacing mode.

conditions, (ii) placing the AICD, (iii) programming the AICD, (iv) performing exposure and recording, and (v) gathering the AICD recordings.

Recording and Checking the Conditions

Two different measuring devices were used to measure the humidity and temperature at different positions in the room. The humidity (15–55%) and temperature (18.7–31.8 °C) were monitored. These variations are negligible on the electric field level [International Electrotechnical Commission, 2013]. Conductivity was always checked before the experiment and had a value range between 0.19 and 0.21 S/m.

Placing the AICD

The phantom required some solid support (Fig. 3) to place the AICD into the solution. In addition, the impedance of the lead and the battery state were inspected before each test. The probe was precisely placed in the middle of the cylindrical part of the phantom, where the induced electric field was homogeneous [Gercek et al., 2017b]. The phantom was grounded, as explained before.

Programming the AICD

Once the AICD was placed into the phantom, the reading probe of the telemetry was fixed near it to establish communication (Fig. 3). Once the good function of the implant was checked, we synchronized it at the same minute and seconds to our records. The PMs and ICDs all were programmed to oversimplify, with an over-range detection window (up to 400 ms), or additional information of the detection features could be obtained from the technical documentation of the cardiac implant. We chose the parameters of disadvantageous scenarios, if not the worst cases, which might differ slightly according to the manufacturer and the model. We deactivated all therapy delivery of the ICD, without inhibiting any detection mode, for the security of the technical board. Once the procedure was finished, the previous records were all erased to avoid any confusion. The telemetry device and any other object in the room were taken out so as not to modify the field. Detailed information about the AICD is given in Table 1.

Performing Exposure and Recording

During tests, no heartbeat signal was applied. Introducing electric cables in such an electric field would perturb the induced electric field and consequently the transfer function between the external electric field and the induced voltage. The only possibility to include these signals would be developing a fiber-optic system, which is a subject of future studies. Security checks were performed before all tests, as described previously. Different exposure levels (up to 100 kV/m in the experimental bench) were applied consecutively to the implanted phantom. The configuration was fixed to 1 min of exposure and one min of non-exposure so we could clearly situate the exposure level that causes dysfunction. The exposure was repeated for different levels up to the memory capacity that the AICD could store as ECG recordings (generally, eight times). The characterization of the electric field in the exposure system in the function of the applied voltage was reported in earlier work by Gercek et al. [2017b]. The start and stop time of exposure, level of application, temperature, and humidity were recorded via the Keysight VEE Pro program, which controls the signal generator (Fig. 1).

Gathering the AICD Recordings

Telemetry (programmer) was set to the communication position to interrogate the AICD inside the phantom. The detection percent and recorded events were noted, and the times of the events were correlated with the exposure time (Fig. 3).

Manufacturers and Sensitivity

Eleven ICDs of eight different types and two manufacturers, as well as 43 PMs of 22 different types and three manufacturers, were included in our study (Table 1). The sensitivity values depended on the manufacturer and the type of AICD (PM or ICD). The maximum sensitivity value was 0.15 mV for Medtronic and 0.2 mV for St. Jude for ICDs. For PMs, 0.2 mV for AAI and 0.5 mV for VVI were the values for bipolar sensing for maximum sensitivity. The nominal sensitivity value was fixed to 0.6 mV for ICDs and to 2 mV for PMs. Other specific configurations may be found elsewhere [Tracy et al., 2013].

RESULTS

All results are given in the field equivalent to a human body. As there was no cardiac signal introduced in the test, we only cover stimulus-dependency and false detection cases. Inhibition of a normal heartbeat or arrhythmia detection is the subject of future work.

The criterion for classifying a reaction of AICD as a dysfunction was any recorded clinical event by the device itself or detection of a certain amount of unusual cardiac signals, as there was no signal

TABLE 2. AICD Reaction Against 50 Hz Electric Field kV/m

50 Hz	Unipolar				Bipolar			
Mode:	AAI		VVI		AAI		VVI	
Sensitivity	Min.	Max.	Min.	Max.	Min.	Max.	Min.	Max.
ICD1	–	–	–	–	Not tested		28	6
ICD2	–	–	–	–	Not tested		43.4	17.4
ICD3	–	–	–	–	Not tested		18.2	5.8
ICD4	–	–	–	–	Not tested		47.1	16.6
ICD5	–	–	–	–	Not tested		43	18.2
ICD6	–	–	–	–	Not tested		17.4	6
ICD7	–	–	–	–	Not tested		24.8	5.8
ICD8	–	–	–	–	Not tested		24	5.8
ICD9	–	–	–	–	Not tested		24.8	5.8
ICD10	–	–	–	–	Not tested		18.6	6.2
ICD11	–	–	–	–	Not tested		19.8	11.6
PM1	5.71	4–24[a]	>245	>245	–	–	–	–
PM2	6.52	4–24[a]	>245	>245	42.2	7.4	>248	>248
PM3	6.52	4–24[a]	>245	>245	33.1	6.6	>248	>248
PM4	8.16	4–24[a]	>245	>245	44.6	6.6	>248	>248
PM5	8.16	4–24[a]	>245	>245	39.7	6.6	>248	>248
PM6	7.35	4–24[a]	>245	>245	33.1	5	>248	>248
PM7	>245	>245[b]	>245	>245	>248	>248	>248	>248

This table mentions the electric field level (kV/m), which causes a dysfunction of the implant at the frequency of 50 Hz. The measurements are made for the unipolar and bipolar mode and for the sensitivities set at the Min and Max values of the implant.

[a]Irreproducible: our system was incapable of delivering ideal sinusoidal voltage at that very low level, adding to that extreme high the sensitivity level, we were not able to reproduce the interference at the same level of the field.

[b]The results obtained for implants PM8 to PM73 are similar to PM7.

TABLE 3. AICD Reaction Against 60 Hz Electric Field kV/m

60 Hz Mode:	Unipolar AAI		VVI		Bipolar AAI		VVI	
Sensitivity	Min	Max.	Min.	Max.	Min	Max.	Min	Max.
ICD1	–	–	–	–	Not tested		33.9	6.6
ICD2	–	–	–	–	Not tested		49.6	20.7
ICD3	–	–	–	–	Not tested		26.3	6.6
ICD4	–	–	–	–	Not tested		55.3	20.7
ICD5	–	–	–	–	Not tested		48.8	21.1
ICD6	–	–	–	–	Not tested		22.3	6.4
ICD7	–	–	–	–	Not tested		28.8	5.8
ICD8	–	–	–	–	Not tested		27.3	6.6
ICD9	–	–	–	–	Not tested		28.1	6.6
ICD10	–	–	–	–	Not tested		19.8	10.7
ICD11	–	–	–	–	Not tested		End of battery	
PM1	4.9	4–24[a]	>200	>200	–	–	–	–
PM2	5.71	4–24[a]	>200	>200	42.2	5.8	>200	>200
PM3	5.71	4–24[a]	>200	>200	33.1	5	>200	>200
PM4	6.52	4–24[a]	>200	>200	44.6	5.8	>200	>200
PM5	7.35	4–24[a]	>200	>200	39.7	9.1	>200	>200
PM6	6.52	4–24[a]	>200	>200	33.1	4.2	>200	>200
PM7	>200	>200[b]	>200	>200	>200	>200	>200	>200

This table mentions the electric field level (kV/m), which causes a dysfunction of the implant at the frequency of 60 Hz. The measurements are made for the unipolar and bipolar mode and for the sensitivities set at the Min and Max values of the implant.
[a]Irreproducible: our system was incapable of delivering ideal sinusoidal voltage at that very low level, adding to that extreme high the sensitivity level, we were not able to reproduce the interference at the same level of the field.
[b]The results obtained for implants PM8 to PM43 are similar to PM7.

induced. If the pacing percentage was around 99% and no event was recorded by the AICD, we concluded that it did not react to EMI. Figure 3 EGM VF (electrogram ventricular fibrillation) would not have any clinical consequences for stimulus-dependency and false detection cases until the very high fields that we tested here, noted as more than 245 kV/m, such as in Tables 2 and 3.

Due to EMI, the ICDs recorded the following episodes: ventricular fibrillation (VF), ventricular tachycardia (VT) (delivering an insignificant amount of 2 or <2 s), noise mode, high-rate heartbeat detection, and VF/VT (St. Jude ICDs could not categorize the induction noise as VT or VF). ICDs, in this case, were asking about more detailed signal definitions; therefore, giving the cardiac signal definition might help the AICD to detect EMI more efficiently.

As for PMs, the inadequate detections were auricular fibrillation or auricular tachycardia, mostly at the dysfunction levels. After that level, false detections occurred of normal (around 60 ppm), a high rate of heartbeats (80–180 ppm), and bradycardia. Figure 4 shows a VF episode detected by ICD. The length of detected events by the AICD caused by fields corresponded almost exactly with the exposure length, which was 58 s to 1 min. In some cases, there were clinically insignificant episodes of extrasystole detected for 2 s before the exposure level reached the dysfunction limit value of the electric field. This is due to the rise and fall time of the field applied and can be neglected for real 50 and 60 Hz electric fields.

All ICDs reacted to a certain level of the electric field, unlike most PMs, which continued to stimulate normally in the case of an absence of heartbeat

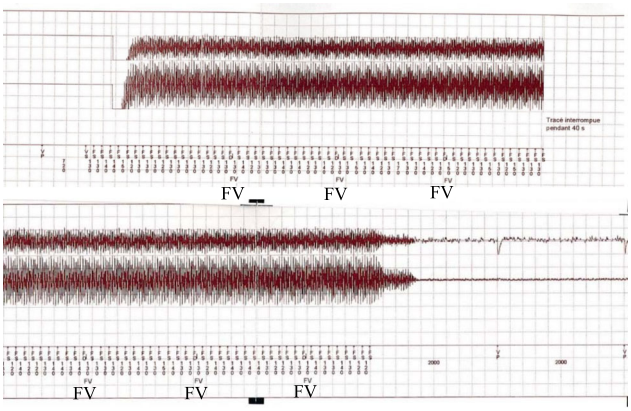

Fig. 4. During in vitro tests with the radiated electric field, the implantable cardioverter-defibrillator (ICDs) memorized the following anomalies: VF (ventricular fibrillation), NR (noise reversion), VTNS (nonsignificant tachycardia). This example concerns EGM (electromyogram) 1-min VF episodes recorded by DAI due to 50-Hz electric field exposure.

signals. None of the 43 PMs reacted in VVI mode up to 248 kV/m at 50 Hz and 200 kV/m at 60 Hz. Thirty-seven PMs did not react in AAI mode, while six PMs showed a dysfunction. The results are summarized in Table 2 for 50 Hz and Table 3 for 60 Hz, respectively.

For a nominal sensitivity configuration, the dysfunction level for the PMs in unipolar AAI mode was higher than the reference levels for public exposure. The same implants were tested in unipolar AAI mode with maximum sensitivity, and all showed dysfunction at a very low level of 2.45 kV/m. Unipolar is thus the mode most convenient for public exposure if it is configured in nominal sensitivity, but there is a potential risk of EMI if the PM is configured as AAI and for maximum sensitivity. The unipolar PM with AAI configuration is not suitable for an occupational environment where the exposure can be up to 10 kV/m or more. However, the PMs with VVI configurations were not affected at all levels of exposure.

For bipolar mode maximum sensitivity, dysfunction limits are always higher than public exposure limits and very close to the limit values that manufacturers guarantee, 5 or 6 kV/m. The tested ICDs were more resistant to 60 Hz than to 50 Hz exposure. Although there are some ICDs perfectly suitable for occupational environments, with maximum sensitivity 7 of 11 presented dysfunctions under 10 kV/m: the low AL limit proposed in 2013/UE/35 [ICNIRP, 1998].

For bipolar-mode nominal sensitivity, all ICDs and PMs are suitable for occupational exposure to electric fields lower than the ALs, except for three ICD models that were disturbed between 17 and 20 kV/m (which is between the low and high AL values). We conclude that unipolar detection is much more susceptible to an electric field interference than the bipolar sensing mode. The sensitivity level plays a major role. The auricular mode is much more vulnerable than ventricular mode for PM. Some PMs did not react at all when configured to VVI up to 248 kV/m; however, they did react in AAI to misinterpretation of the EMI signal with tachycardia or fibrillation. Detection interpretation by the device under test and the dysfunction level vary depending on the type of AICD and the manufacturer. For instance, a study by Korpinen et al. [2012] involved 31 PM tested at 50 Hz, and about 7 kV/m showed that only one PM reacted to EMI in unipolar mode DDD (Dual-chamber pacing and sensing, with atrial synchronous ventricular pacing).

DISCUSSION

It is crucial to highlight that these results were obtained for highly disadvantageous scenarios: close to or worst-case in given conditions. Indeed, our results indicate field levels for which there is a potential risk that devices will have a dysfunction caused by EMI, which may lead to a clinically significant event. However, it may not systematically imply health consequences, and effects are always reversible once the AICD is no longer under exposure. We also observed rare cases where EMI caused AICDs to switch into noise mode, which means that they continued to deliver the standard heartbeat.

We excluded 17 AICDs that ran out of battery power after the telemetry warning indicating a critical state of charge. (Before getting to this stage of charge, the patient was alerted by a clearly noticeable vibration or sound months before, and if the battery or AICD is not changed, pacing functions can even stop, so we did not study that extreme case.)

The chamber configuration of the AICD might also affect the electric field level that may induce dysfunction. From the 110 ICD patients that were tested in Aachen [Napp et al., 2014], none of them were in auricular mode AAI (atrial-inhibited pacing mode), while some of them were in DDD mode. In addition, we did some tests in DDD configuration on a small random sample of AICDs. However, we did not find any failure below the ones that had already been found as AAI or VVI, as expected. The signal discrimination algorithms were working more efficiently with two leads than one at such low frequencies and laboratory conditions. Moreover, a group of AICDs also was tested in a state of minimal sensitivity, and none of them showed any reaction. So

as not to overwhelm the numerous results, we will not discuss those tests.

We experimentally tested 54 AICDs against 50 and 60 Hz, with a statistically significant number of devices. Seven different types of over 11 ICDs and 28 different types of 43 PMs were tested. The design of the experimental bench and phantom was done considering a worst-case exposure, including a grounded human body (which is not common in daily life and even less probable in occupational exposure). As the worker will wear isolated shoes, in theory, there is no risk of false detection of arrhythmia. In the case of a stimulus-dependent patient, risk is minimal to work in occupational exposure if bipolar AICDs are configured at nominal sensitivity. The inhibition of the detection of a pathological incident such as VF or VT should be studied by injecting a cardiac signal.

The level of interference is close to in situ as well as in vivo findings in the literature [International Electrotechnical Commission, 2007; Gercek et al., 2017b], and the differences might be coming from different models and testing methodologies. For example, one test was completed under real 400 kV lines [Korpinen et al., 2014], and another one was a current injection in vivo [Pavlicek et al., 2017]. In this paper, we proposed an in vitro approach to test the AICDs in electric fields with a cost-effective test bench that may help to build a risk assessment for workers bearing cardiac implants in the frame of the family standard CENELEC 50527.

More investigations with heartbeat signals are necessary to ascertain whether the cardiac signals are drowned in noise, so that patients living with pathology are not simply ignored for treatment because of EMI.

CONCLUSION

Forty-three PMs and 11 ICDs were tested against 50- and 60 Hz electric fields up to 248 and 200 kV/m, respectively. On the basis of the results of this study, there appears to be no risk of EMI for a false treatment for stimulus-dependent patients in public places with PMs, unless the device is configured with unipolar maximum sensitivity. When AICDs are configured with bipolar maximum sensitivity or unipolar nominal sensitivity, there appears to be no risk of EMI for the same cases due to public exposure, but occupational exposure may present some degree of concern. However, there appears to be no risk for AICDs configured in bipolar mode with nominal sensitivity in occupational environments compliant with low ALs according to EU directives, although a very slight risk exists for high ALs for a few ICDs tested. The influence of ungrounded phantoms and heartbeat signals may be the subject of future studies, which will clarify two other cases that could not be studied: inhibition of heartbeat signal or arrhythmia detection (in the case where a patient has an arrhythmia while EMI occurs).

ACKNOWLEDGMENT

Our thanks to Pr Sadoul from the cardiology department of CHRU Nancy for providing explanted AICDs for our research.

REFERENCES

Abbott. 2017. Battery performance alert: A tool for improved patient management for devices under battery advisory. Available from: https://www.cardiovascular.abbott/com [Last accessed 20 October 2019].

Beebe DJ. 1993. Signal conversion. In: Tompkins W, editor, Biomedical Digital Signal Processing. Englewood Cliffs, NJ: Prentice-Hall. pp 61–74.

CRDM Technical Services. 2014. Explanation of implantable devices at end of service. Standard guidance letter. Available from: https://wwwp.medtronic.com [Last accessed 20 October 2019].

Deno DW. 1977. Currents induced in the human body by high-voltage transmission line electric field: Measurement and calculation of distribution and dose. IEEE Trans Power App System 96:1517–1527.

Directive 2013/35/UE. 2013. Directive 2013/35/UE of the European Parliament and the Council. On the minimum health and safety requirements regarding the exposure of workers to the risks arising from physical agents (electromagnetic fields).

Dyrda K, Nguyen DH, Thibault B, Khairy P, Venier S, Talajic M, Dubuc M, Macle L, Mondesert B, Guerra PG, Rivard L, Plante M, Ostiguy G. 2015. Interference resistance of pacemakers and defibrillators to 60 Hz electric fields. Can J Cardiol 31:S233–S234.

EN 50527-1. 2016. Procedure for the assessment of the exposure to electromagnetic fields of workers bearing active implantable medical devices—Part 1: General.

EN 50527-2-1. 2017. Procedure for the assessment of the exposure to electromagnetic fields of workers bearing active implantable medical devices. Specific assessment for workers with cardiac pacemakers.

EN 50527-2-2. 2018. Procedure for the assessment of the exposure to electromagnetic fields of workers bearing active implantable medical devices. Specific assessment for workers with cardioverter defibrillators (ICDs).

Gabriel C, Peyman A, Grant EH. 2009. Electrical conductivity of tissue at frequencies below 1 MHz. Phys Med Biol 54:4863–4878.

Gercek C, Kourtiche D, Nadi M, Magne I, Schmitt P, Souques M, Roth P. 2017a. An in vitro cost-effective test bench for active cardiac implants, reproducing human exposure to electric fields 50/60 Hz. Int J Smart Sensing Intell Syst 10:1–17.

Gercek C, Kourtiche D, Nadi M, Magne I, Schmitt P, Souques M. 2017b. Computation of pacemakers immunity to 50 Hz

electric field: Induced voltages 10 times greater in unipolar than in bipolar detection mode. Bioengineering 4:1–19.

International Commission on Non-Ionizing Radiation Protection (ICNIRP). 1998. Guidelines for limiting exposure to time-varying electric, magnetic, and electromagnetic fields (up to 300 GHz). Health Phys 74:494–522.

International Commission on Non-Ionizing Radiation Protection (ICNIRP). 2010. Guidelines for limiting exposure to time-varying electric and magnetic fields (1 Hz to 100 kHz). Health Phys 99:818–836.

International Electrotechnical Commission (IEC 62226-3-1). 2007. Exposure to electric or magnetic fields in the low and intermediate frequency range—Methods for calculating the current density and internal electric field induced in the human body—Part 3-1: Exposure to electric fields—Analytical and 2D numerical models.

International Electrotechnical Commission. 2013. IEC technical committee 106: Methods for the assessment of electromagnetic and electromagnetic fields associated with human exposure. 61786-1: Measurement of DC magnetic, AC magnetic and AC electric fields from 1 Hz to 100 kHz regarding exposure of human beings. Part 1.

Jeremias A, Brown DL. 2010. Cardiac Intensive Care. Oxford, UK: Elsevier Health Sciences. pp 225–232.

Joosten S, Pammler K, Silny J. 2009. The influence of anatomical and physiological parameters on the interference voltage at the input of unipolar cardiac pacemakers in low frequency electric fields. Phys Med Biol 54:591–609.

Katrib J, Nadi M, Kourtiche D, Magne I, Schmitt P, Souques M, Roth P. 2013. In vitro assessment of the immunity of implantable cardioverter-defibrillators to magnetic fields of 50/60 Hz. Physiol Meas 34:1281–1292.

Korpinen L, Kuisti H, Elovaara J, Virtanen V. 2012. Cardiac pacemakers in electric and magnetic fields of 400-kv power lines. Pacing Clin Electrophysiol 35:422–430.

Korpinen L, Kuisti H, Elovaara J, Virtanen V. 2014. Implantable cardioverter defibrillators in electric and magnetic fields of 400 kv power lines: Implantable cardioverter defibrillators in fields. Pacing Clin Electrophysiol 37:297–303.

Motrescu VC, van Rienen U. 2005. Computation of currents induced by ELF electric fields in anisotropic human tissues using the finite integration technique (FIT). Adv Radio Sci 3:227–231.

Napp A, Joosten S, Stunder D, Knackstedt C, Zink M, Bellmann B, Marx N, Schauerte P, Silny J. 2014. Electromagnetic interference with implantable cardioverter-defibrillators at power frequency: An in vivo study. Circulation 129:441–450.

Orgeron GM, James CA, Te Riele A, Tichnell C, Murray B, Bhonsale A, Kamel IR, Zimmerman SL, Judge DP, Crosson J, Tandri H, Calkins H. 2017. Implantable cardioverter defibrillator therapy in arrhythmogenic right ventricular dysplasia/cardiomyopathy: Predictors of appropriate therapy, outcomes, and complications. J Am Heart Assoc 6:1–10.

Pavlicek V, Wintrich J, Mahfoud F, Klingel K, Kandolf R, Boehm M, Kindermann I, Ukena C. 2017. Implanted cardioverter defibrillator (ICD) therapy in patients with suspected myocarditis: Time of implantation and occurrence of ventricular arrhythmias. Europace 19:128.

Schlimp CJ, Breiteneder M, Seifert J, Lederer W. 2007. Interference of 16.7-Hz electromagnetic fields on measured electrocardiogram. Bioelectromagnetics 28:402–405.

Stuchly MA, Kavet R. 2005. Numerical modeling of pacemaker interference in the electric-utility environment. IEEE Trans Dev Mat Reliab 5:481–487.

Tracy CM, Epstein AE, Darbar D, DiMarco JP, Dunbar SB, Estes NAM, Ferguson TB, Hammill SC, Karasik PE, Link MS, Marine JE, Schoenfeld MH, Shanker AJ, Silka MJ, Stevenson LW, Stevenson WG, Varosy PD. 2013. 2012 ACCF/AHA/HRS focused update incorporated into the ACCF/AHA/HRS 2008 guidelines for device-based therapy of cardiac rhythm abnormalities. J Am Coll Cardiol 61:e6–e75.

Valentin J. 2002. Basic anatomical and physiological data for use in radiological protection: Reference values. A report of age-and gender-related differences in the anatomical and physiological characteristics of reference individuals. ICRP Publication 89. Ann ICRP 32:5–265.

Webster JG, Clark JW, editors, 2010. Medical instrumentation: Application and Design, 4th ed. Hoboken, NJ: John Wiley & Sons. p 736.

Weiland T. 1977. A discretization model for the solution of Maxwell's equations for six-component fields. Arch Elektron Uebertrag 31:116–120.